Separation Science and Technology
Publication details, including instructions for authors and subscription information:
http://www.informaworld.com/smpp/title~content=t713708471

Outlet Stream Swing Simulated Moving Bed: Separation and Regeneration Regions Analysis

Pedro Sá Gomes[a]; Alírio E. Rodrigues[b]
[a] CAT Catalytic Center, ITMC, RWTH Aachen University, Aachen, Germany [b] Laboratory of Separation and Reaction Engineering, Associate Laboratory LSRE/LCM, Department of Chemical Engineering, Faculty of Engineering, University of Porto, Porto, Portugal

Online publication date: 29 November 2010

To cite this Article Gomes, Pedro Sá and Rodrigues, Alírio E.(2010) 'Outlet Stream Swing Simulated Moving Bed: Separation and Regeneration Regions Analysis', Separation Science and Technology, 45: 16, 2259 — 2272
To link to this Article: DOI: 10.1080/01496395.2010.497525
URL: http://dx.doi.org/10.1080/01496395.2010.497525

Separation Science and Technology, 45: 2259–2272, 2010

ISSN: 0149-6395 print/1520-5754 online
DOI: 10.1080/01496395.2010.497525

Taylor & Francis
Taylor & Francis Group

Outlet Stream Swing Simulated Moving Bed: Separation and Regeneration Regions Analysis

Pedro Sá Gomes[1] and Alírio E. Rodrigues[2]
[1]*CAT Catalytic Center, ITMC, RWTH Aachen University, Aachen, Germany*
[2]*Laboratory of Separation and Reaction Engineering, Associate Laboratory LSRE/LCM, Department of Chemical Engineering, Faculty of Engineering, University of Porto, Porto, Portugal*

In this work, the Outlet Stream Swing (OSS) non-conventional operation technique is compared with a classical Simulated Moving Bed (SMB) unit, for the separation of a racemic mixture of guaifenesin. A methodic approach, based on the complete separation and regeneration regions, is used to evaluate the performance of the OSS *extract-raffinate*, as well as the OSS *raffinate-extract*, operating strategies with the classical SMB in terms of purity, productivity and eluent consumption requirements. The variants of the OSS technique: OSS *extract-0* and OSS *raffinate-0* are presented, simulated, and used not only to introduce more simplistic OSS modes of operation, but also to better understand the influence of specific OSS operating parameters. The experimental validation of OSS *extract-0*, operated by means of the FlexSMB-LSRE® unit, is also presented as part of this work, demonstrating the potential, as limitations, of such operating techniques.

Keywords Chiralpak AD; FlexSMB-LSRE®; guaifenesin; OSS; Outlet Stream Swing; Simulated Moving Bed; SMB

INTRODUCTION

The Simulated Moving Bed (SMB) is an original separation technique which appeared to solve several of the problems associated with solid phase motion (particle attrition and wall abrasion, particle size redistribution, increase in pressure drop), usually observed when operating under the continuous countercurrent adsorptive separation processes, the so-called True Moving Bed (TMB). The origins of SMB can be traced back to the early 1960s, and its first relevant industrial implementation to the Sorbex® processes by Universal Oil Products-USA (1,2). Since its introduction, the SMB technology has been successfully applied, first to various large petrochemical separations, such as: the *p*-xylene separation from its C_8 isomers (with 88 Parex units licensed by UOP LLC-USA since 1971, ranging from 21 to 1600 kton · year^{-1} of *p*-xylene; 8 Eluxyl units licensed by Axens (IFP)-France since 1995, with capacities ranging from 180 to 750 kton · year^{-1}; 2 Aromax units licensed by Toray Industries Inc.-Japan since 1973, with a range of about 200 kton · year^{-1}); *n*-paraffins from branched and cyclic hydrocarbons (with 28 Molex units licensed by UOP LLC-USA); the sugar processing industry (Sarex process by UOP LLC-USA; more than 90 SMB and Improved-SMB plants by FAST - ''Finnsugar Applexion Separation Technology'', now Novasep-France; and Amalgamated Sugar Co.-USA) and later, in the pharmaceutical and fine chemical industries (with more than 50 units currently installed, mainly by Novasep-France, Knauer GmbH-Germany, Bayer BTS-Germany, SepTor Technologies BV-Netherlands part of Outotec Oyj-Finland, and ChromaCon AG-Switzerland) (3–6).

This late demand on the SMB technique, directly linked to a considerable research effort, led to the formulation of quite different operation modes since the original patent, as reviewed elsewhere (4,7). From these so-called non-conventional operating strategies, one can emphasize those based in the periodic modulation of inlet/outlet streams flow rates, such as:

- the Partial-Feed (8,9), in which the inlet feed flow rate varies along the time compensated by the raffinate flow rate; or in the limit, by varying all internal flow rates, the PowerFeed (10–13);
- the Partial-Discard (or partial withdraw) (9,14), performed by a partial collection in the extract and/or raffinate streams; the fraction that has not been ''collected'' can be recycled back to the feed after a possible concentration step (3,15);
- the ISMB (Improved, also called intermittent, SMB) mode of operating, commercialized by the Nippon Rensui Co. (Tokyo, Japan) (16), with two different stages: a first step, where the unit is operated as a conventional SMB but without any flow in section IV; and in the second step,

Received 1 February 2010; accepted 27 May 2010.
Present address: CAT Catalytic Center, ITMC, RWTH Aachen University, Worringerweg 1, 52074 Aachen, Germany.
Address correspondence to Alírio E. Rodrigues, Department of Chemical Engineering, Faculty of Engineering of the University of Porto, Rua Dr. Roberto Frias, 4200-465 Porto, Portugal. Tel.: +351 22 5081671; Fax: +351 22 5081674. E-mail: arodrig@fe.up.pt

where the inlet and outlet ports are closed and the internal flow through the four sections allowing the concentration profiles to move to adjust their relative position with respect to the outlet ports (7,17).

A considerable performance improvement has been noted by the application of such techniques. However, while the partial feed strategy has been considerably studied over time, resulting in significant productivity improvements, the analysis of a similar eluent/desorbent flow rate variation has not been particularly addressed.

Based on this statement, and in part inspired on the partial discard as ISMB techniques, a new operation technique was introduced before: the Outlet Streams Swing (OSS) (18,19). This operating mode assumes that both the extract and the raffinate flow rates can be varied over time, but keeping the same overall operating parameters, i.e., the average section flow rates over a switching time period are the same as in a classic SMB. In this way, a reduction (or closure) of the extract, or raffinate flow rate over an initial fraction of the switching time is then compensated by an increase of this same flow rate over the remaining part of the switching time period, or vice-versa. The technique can be employed varying both the extract and raffinate flow rates at the same time, operating with extract high and raffinate low flow rates, during the first fraction of the switching time period, followed by extract low and raffinate high flow rates (Fig. 1), or vice-versa (Fig. 2).

From both strategies shown in Figs. 1 and 2, one can observe that section II (between the extract and feed ports) and section III (between the feed and raffinate ports) do not suffer any changes over time (are maintained at constant flow rates) and thus, the eluent/desorbent flow rate fluctuate to amortize the effect of extract or raffinate flow rate variations, a sort of ''partial eluent'' strategy. In fact, only section I (between the eluent and extract ports) and section IV (limited by the raffinate and eluent ports) suffer the flow rates variations. Considering that each step is performed for 50% of the switching time the name 50–50% OSS extract-raffinate is given for the strategy in Fig. 1 and 50–50% OSS raffinate–extract for the operating scheme in Fig. 2.

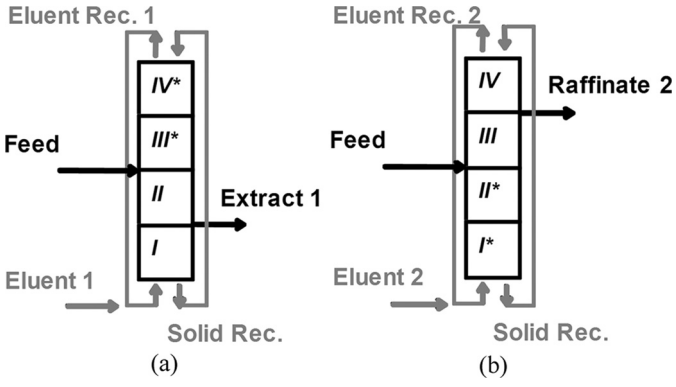

FIG. 1. OSS *extract-raffinate* strategy, (a) the first fraction of the switching time, (b) the remaining part of the switching time period, equivalent TMB scheme (adapted (18)).

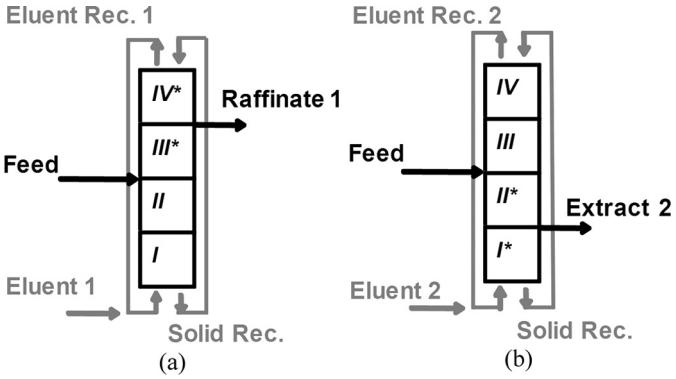

FIG. 2. OSS *raffinate-extract* strategy, (a) the first fraction of the switching time, (b) the remaining part of the switching time period, equivalent TMB scheme (adapted (18)).

In this work, the potential of such technique is demonstrated by means of detailed analysis to its respective separation and regeneration regions, applied here to the resolution of a racemic mixture of guaifenesin enantiomers. Different variants of this technique are also presented, simulated, and analyzed, concluding with its experimental validation.

THEORETICAL SECTION

Case Study

The resolution of guaifenesin enantiomers by means of Chiralpak AD (amylose tris-(3,5 dimethylphenylcarbamate coated onto 20 μm silica-gel, provided by Chiral Technologies Europe-France), with a *n*-heptane/ethanol mixture at 85/15 in volumetric percentage as mobile phase, was chosen as a case study for this work. The information related to this system adsorption equilibrium was determined by frontal analysis at a preparative scale and fitted by a Langmuir type isotherm as presented elsewhere (20).

$$q_i^{eq} = \frac{q_m K_i \overline{C_{p_i}}}{1 + \sum_{l=1}^{2} K_l \overline{C_{p_l}}} \tag{1}$$

where, $\overline{C_{p_i}}$, is the *i* component particle average pore concentration in $g \cdot l^{-1}$; q_i^{eq}, is the adsorbed phase concentration in $g \cdot l_{cat}^{-1}$ in equilibrium with the average pore concentration; q_m, is the total adsorbent capacity in $g \cdot l_{cat}^{-1}$ and K_i, the adsorption isotherm parameters in $l \cdot g^{-1}$. The fitting

TABLE 1
Multicomponent adsorption isotherm parameters

q_m [g · l$_{cat}^{-1}$]	K_A [l · g^{-1}]	K_B [l · g^{-1}]
106.759	0.065	0.056

parameters, obtained by the Levenberg-Marquardt algorithm, are presented in Table 1.

The mass transfer resistances for this system was represented by the internal mass transfer coefficient, k_{int_i}, obtained by means of a Linear Driving Force (LDF) approximation, $k_{\text{int}_i} = \frac{5\varepsilon_p D_{m_i}}{\tau r_p}$ (21); with, D_{m_i}, as the free molecular diffusivity and τ, the particle tortuosity factor, calculated from the approximation $\tau = \frac{(2-\varepsilon_p)^2}{\varepsilon_p}$; with ε_p the particle porosity and r_p the particle radius. The solute molecular diffusivity was estimated by the Wilke–Chang (22) equation extended to mixed solvents by Perkins and Geankoplis (23) $D_{m_i} = 7.4 \times 10^{-8} T \frac{\sqrt{\phi M}}{\mu V_{m_i}^{0.6}}$; where T represents the absolute temperature; μ the mobile phase viscosity, evaluated according to Teja and Rice (24) method for the liquid mixture; V_{m_i} is the adsorbate molar volume at its normal boiling temperature estimated by the Le Bas method; and ϕM was obtained from $\phi M = x_A \phi_A M_A + x_B \phi_B M_B$, where x_i are the molar fractions, M_i the molar masses, and ϕ_i are the association factors constants which account for the solute-solvent interactions. The molecular diffusivity was assumed to be the same for both enantiomers, and thus, the internal mass transfer coefficient, $k_{\text{int}_i} = 0.20\,\text{cm} \cdot \text{min}^{-1}$, equal for both enantiomers (20).

Modeling and Design Strategies

One can argue that an SMB unit is no more than the practical implementation of the continuous countercurrent TMB process. Consequently, the equivalence between the TMB and a hypothetical SMB with an infinite number of columns can be used in the modeling and design of real SMB units (6). However, modeling an SMB unit by means of the model of its equivalent TMB unit, will just present a reasonable agreement with the real unit when a large number of columns per section are considered. Since this is not the case of this work, one will model the SMB unit by means of a discontinuous approach, considering a sequence of columns, described by the usual system equations for an adsorptive fixed bed (each column k), which inlets change over time, modeling in this way the real ports shift.

The SMB model approach, used to simulate this particular separation, relies on the LDF approximation mentioned before, set in terms of fluid phase concentration $(C_{b_{i,k}} - \overline{C_{p_{i,k}}})$.

Mass Balances

Obtained by performing a mass balance to a volume element of the column k,

$$\frac{\partial C_{b_{i,k}}}{\partial t} = D_{b_k} \frac{\partial^2 C_{b_{i,k}}}{\partial z^2} - u_j^* \frac{\partial C_{b_{i,k}}}{\partial z} - \frac{(1-\varepsilon_b)}{\varepsilon_b} \frac{3}{r_p} k_{\text{int}_i} (C_{b_{i,k}} - \overline{C_{p_{i,k}}}) \tag{2}$$

and similarly for the particle mass balance,

$$\varepsilon_p \frac{\partial \overline{C_{p_{i,k}}}}{\partial t} + (1-\varepsilon_p) \frac{\partial q_{i,k}^{eq}}{\partial t} = \frac{3}{r_p} k_{\text{int}_i} (C_{b_{i,k}} - \overline{C_{p_{i,k}}}) \tag{3}$$

Initial Conditions

$$t = 0 : C_{b_{i,k}}(z,0) = \overline{C_{p_{i,k}}}(z,0) = 0 \tag{4a,b}$$

Boundary Conditions

The Danckwerts boundary conditions (25), at the inlet of column ($z = 0$) as at the column exit ($z = L_k$) for ($t > 0$), are set to each column k,

$$z = 0 : D_{b_k} \left.\frac{\partial C_{b_{i,k}}}{\partial z}\right|_{z=0} = u_j^* (C_{b_{i,k}}|_{z=0} - C_{b_{i,k}}^0) \tag{5}$$

$$z = L_k : \left.\frac{\partial C_{b_{i,k}}}{\partial z}\right|_{z=L_k} = 0 \tag{6}$$

With z and t representing the axial and time coordinates, respectively; L_k the column k length; ε_b the bulk porosity; D_b the axial dispersion coefficient, and u_j^* the section j fluid interstitial velocity.

Nodes Equations

The interstitial fluid velocities, and inlet concentrations in each section j are calculated from the inlet and outlet nodes balances:

$$\text{Eluent (E) node} : u_I^* = u_{IV}^* + u_E \tag{7a}$$

$$\text{Extract (X) node} : u_{II}^* = u_I^* - u_X \tag{7b}$$

$$\text{Feed (F) node} : u_{III}^* = u_{II}^* + u_F \tag{7c}$$

$$\text{Raffinate (R) node} : u_{IV}^* = u_{III}^* - u_R \tag{7d}$$

Due to the switch of inlet and outlet lines, the boundary conditions to a certain column are not constant during a whole cycle but change after a period equal to the switching time t_s. Since the model equations are set to each

column k, one will obtain the concentration of i species in the beginning of each section j, $C^0_{b_{i,k}}$, from the following node mass balances:

For $t=0$ to t_s:

$$k=1: C_{b_{i,\left(\sum_{j=I}^{IV} n_j\right)}}\Big|_{z=L_{\sum_{j=I}^{IV} n_j}} = \frac{u^*_I}{u^*_{IV}} C^0_{b_{i,1}} - \frac{u_E}{u^*_{IV}} C^E_i \quad (8a1)$$

$$k=2 \text{ to } k=(n_I+n_{II}): C_{b_{i,(k-1)}}\Big|_{z=L_{(k-1)}} = C^0_{b_{i,k}} \quad (8a2)$$

$$k=(n_I+n_{II}+1): C_{b_{i,(n_I+n_{II})}}\Big|_{z=L_{(n_I+n_{II})}} = \frac{u^*_{III}}{u^*_{II}} C_{b_{i,(n_I+n_{II}+1)}} - \frac{u_F}{u^*_{II}} C^F_i \quad (8a3)$$

$$k=(n_I+n_{II}+2) \text{ to } k=\sum_{j=I}^{IV} n_j: C_{b_{i,(k-1)}}\Big|_{z=L_{(k-1)}} = C^0_{b_{i,k}} \quad (8a4)$$

For $t=t_s$ to $2t_s$:

$$k=1: C_{b_{i,\left(\sum_{j=I}^{IV} n_j\right)}}\Big|_{z=L_{\left(\sum_{j=I}^{IV} n_j\right)}} = C^0_{b_{i,1}} \quad (8b1)$$

$$k=2: C_{b_{i,1}}\Big|_{z=L_1} = \frac{u^*_I}{u^*_{IV}} C^0_{b_{i,2}} - \frac{u_E}{u^*_{IV}} C^E_i \quad (8b2)$$

$$k=3 \text{ to } k=(n_I+n_{II}+1): C_{b_{i,(k-1)}}\Big|_{z=L_{(k-1)}} = C^0_{b_{i,k}} \quad (8b3)$$

$$k=(n_I+n_{II}+2): C_{b_{i,(n_I+n_{II}+1)}}\Big|_{z=L_{(n_I+n_{II}+1)}} = \frac{u^*_{III}}{u^*_{II}} C^0_{b_{i,(n_I+n_{II}+2)}} - \frac{u_F}{u^*_{II}} C^F_i \quad (8b4)$$

$$k=(n_I+n_{II}+3) \text{ to } k=\sum_{j=I}^{IV} n_j: C_{b_{i,(k-1)}}\Big|_{z=L_{(k-1)}} = C^0_{b_{i,k}} \quad (8b5)$$

This set of equations continues to progress in a similar way (shifting one column per t_s), until $t=t_s\sum_{j=I}^{IV} n_j$, repeating then from the first switch.

Performance Parameters

The performance of the SMB unit for a given separation is usually characterized by purity, recovery, and productivity per the amount of adsorbent volume (6). The definitions of all these performance parameters, for the case of a binary mixture, are given below:

Purity (%) of the more retained (A) species in extract and the less retained one (B) in the raffinate stream, over a complete cycle, from t to $t+t_s\sum_{j=I}^{IV} n_j$:

$$PU_X = \frac{\int_t^{t+t_s\sum_{j=I}^{IV} n_j} C^X_{b_A} dt}{\int_t^{t+t_s\sum_{j=I}^{IV} n_j} C^X_{b_A} dt + \int_t^{t+t_s\sum_{j=I}^{IV} n_j} C^X_{b_B} dt} \quad (9a)$$

$$PU_R = \frac{\int_t^{t+t_s\sum_{j=I}^{IV} n_j} C^R_{b_B} dt}{\int_t^{t+t_s\sum_{j=I}^{IV} n_j} C^R_{b_A} dt + \int_t^{t+t_s\sum_{j=I}^{IV} n_j} C^R_{b_B} dt} \quad (9b)$$

Recovery (%) of more retained (A) species in extract and the less retained one (B) in raffinate stream, again over a complete cycle:

$$RE_X = \frac{\int_t^{t+t_s\sum_{j=I}^{IV} n_j} C^X_{b_A} dt \cdot Q_X}{t_s\sum_{j=I}^{IV} n_j \cdot Q_F C^F_A} \quad (10a)$$

$$RE_R = \frac{\int_t^{t+t_s\sum_{j=I}^{IV} n_j} C^R_{b_B} dt \cdot Q_R}{t_s\sum_{j=I}^{IV} n_j \cdot Q_F C^F_B} \quad (10b)$$

the productivity per total volume of adsorbent $\frac{g}{l_{adsorbent}\cdot day}$:

$$PR_X = \frac{\int_t^{t+t_s\sum_{j=I}^{IV} n_j} C^X_{b_A} dt \cdot Q_X}{t_s\left(\sum_{j=I}^{IV} n_j\right)^2 V_c(1-\varepsilon_b)} = \frac{RE_X Q_F C^F_A}{V_c(1-\varepsilon_b)\sum_{j=I}^{IV} n_j} \quad (11a)$$

$$PR_R = \frac{\int_t^{t+t_s\sum_{j=I}^{IV} n_j} C^R_{b_B} dt \cdot Q_X}{t_s\left(\sum_{j=I}^{IV} n_j\right)^2 V_c(1-\varepsilon_b)} = \frac{RE_R Q_F C^F_B}{V_c(1-\varepsilon_b)\sum_{j=I}^{IV} n_j} \quad (11b)$$

The number of columns as its volume (and thus the amount of adsorbent), will not be changed along this work. Consequently, one can simplify the productivity analysis by direct comparison of the maximum feed flow rate allowable in the vertex of the separation region ($Q^*_{III}-Q^*_{II}=Q_F$). A similar approach can be used to induce about the eluent recovery, but, in this case, referring to the lower solvent consumption in the regeneration region ($Q^*_I-Q^*_{IV}=Q_E$).

Numerical Solution

All the following simulations were obtained by solving the mathematical model with gPROMS software package

(version 3.0.4) from Process System Enterprise (UK). The numerical method used was based on the Orthogonal Collocation in Finite Elements with an axial discretization in 40 finite elements, with two interior collocation points. An absolute and relative tolerance of 10^{-5} was set.

Performance Analysis

Separation Region Analysis

The design procedure used to determine the operating conditions for a resolution of a racemic mixture of guaifenesin, by means of an SMB unit operating in the classical mode, was presented before (20), and used here to establish the limiting conditions, namely $Q^*_{I_{\max}}$ and $Q^*_{IV_{\min}}$, for the separation region analysis. To account for the mass transfer resistances when drawing the separation region, one can make use of the SMB model stated in the previous section and run successive simulations of different $(Q^*_{II} \times Q^*_{III})$ pairs. To do so, one should consider significantly higher values for Q^*_I and lower values for Q^*_{IV}, than the ones predicted by the Triangle Theory (26), to guarantee that the flow rates in the regeneration region do not influence the shape and size of the separation region, as stated by the Separation Volume concept (27). This procedure was in fact used to perform the separation region analysis for the pure 50–50% OSS *raffinate-extract* and *extract-raffinate* running successive simulations for different $(Q^*_{II} \times Q^*_{III})$ pairs with constant $Q^*_I = 44.0\,\text{ml}\cdot\text{min}^{-1}$, $Q^*_{IV} = 32.0\,\text{ml}\cdot\text{min}^{-1}$, and $t_s = 2.57\,\text{min}$ and the SMB unit parameters considered, from the FlexSMB-LSRE® unit (detailed later), presented in Table 2.

The separation regions obtained are shown in Fig. 3.

From Fig. 3, one can observe that while the SMB classic and the OSS *extract-raffinate* (OSS *XR*) strategy separation regions are almost superposed, the separation region of the OSS *raffinate-extract* (OSS *RX*) appears to be slightly larger than the previous two and thus allowing, to some extent, higher productivities or higher purities for a given operating point.

Regeneration Region Analysis

In the case of the regeneration region analysis for the pure 50–50% OSS *raffinate-extract* and *extract-raffinate*, the analysis was performed again by running successive simulations, now for different $(Q^*_I \times Q^*_{IV})$ pairs with constant $Q^*_{II} = 36.2\,\text{ml}\cdot\text{min}^{-1}$, $Q^*_{III} = 37.1\,\text{ml}\cdot\text{min}^{-1}$ and $t_s = 2.57\,\text{min}$, Fig. 4.

The pair $(Q^*_{II} \times Q^*_{III})$ was chosen according to an operating point positioned within the separation region presented before (Fig. 3), and detailed elsewhere (20).

TABLE 2
Experimental operating conditions of the FlexSMB-LSRE® unit, geometrical factors and feed concentration

$n_j = [1\ 2\ 2\ 1]$	$\varepsilon_b = 0.4$
$L_c = 10\,\text{cm}$	$C_i^F = 2.0\,\text{g}\cdot\text{l}^{-1}$
$d_c = 2.0\,\text{cm}$	$d_p = 20\,\mu\text{m}$

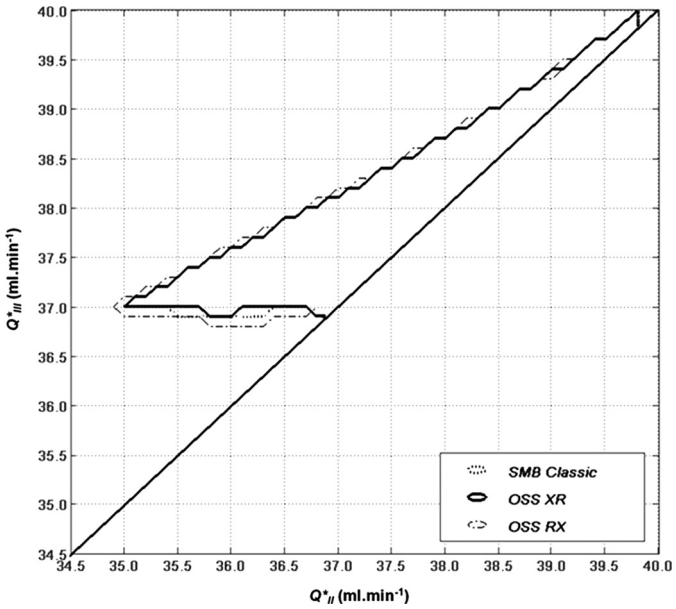

FIG. 3. Separation region for classic SMB and 50–50% OSS strategies: *extract-raffinate* (OSS *XR*) and *raffinate-extract* (OSS *RX*), step of $0.100\,\text{ml}\cdot\text{min}^{-1}$ for both Q^*_{II} and Q^*_{III}; minimum purity in both extract and raffinate streams of 99.75%.

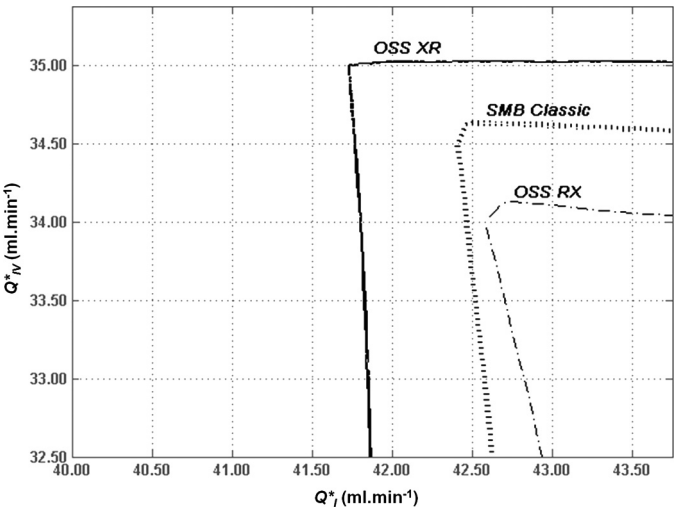

FIG. 4. Regeneration region for classic SMB and 50–50% OSS strategies: *extract-raffinate* (OSS *XR*) and *raffinate-extract* (OSS *RX*) step of $0.125\,\text{ml}\cdot\text{min}^{-1}$ and $0.250\,\text{ml}\cdot\text{min}^{-1}$ for Q^*_I and Q^*_{IV}, respectively; minimum purity in both extract and raffinate streams of 99.75%.

From Fig. 4, it can be observed that the OSS *extract-raffinate* operating strategy is now considerably better than the SMB classic, and this last quite better than the OSS *raffinate-extract* (regeneration region area: OSS *extract-raffinate* > SMB > OSS *raffinate-extract*), an opposite conclusion than the one obtained from the separation region analysis. However, the differences between both OSS strategies and the classic operating SMB mode observed in Fig. 4 (regeneration region analysis) are quite larger than the ones observed in Fig. 3 (separation region analysis) and thus, stating the OSS operating mode as a sort of partial eluent strategy (by opposition with the partial feed strategy). In fact, one expects that the OSS mode of operation will play a more relevant role in eluent consumption (or eluent recovery duties) studies than in the productivity optimization.

If the objective is to improve the productivity values (for instance, by increasing the feed flow rate), the OSS *raffinate-extract* strategy will better suit the purpose. It is interesting to note that a similar conclusion was achieved by Kawajiri and Biegler (12) when performing the maximization of the feed flow rate (productivity or outlet purity for a given recovery value requirement), keeping constant the section flow rates (''Constant zone velocities'') and variable inlet and outlets streams. These authors performed what can be named as a sort of partial feed coupled with the OSS technique, and by optimization found the basics for the modus operandi of a 40%–60% OSS *raffinate-extract* operating strategy. For instance, see Fig. 4 of Kawajiri and Biegler (12), where, and apart from the feed flow rate influence on the other ports, it can be noted that the extract port is closed for roughly 40% of the initial part of the switching time period, and the remaining part opened, while the opposite can more or less be observed for the raffinate port. The eluent stream is higher in the first part of the switching time period and then decreased over the second part. Such procedure is in fact quite similar to the one found in this work for the maximization of productivity.

On the other hand, if the objective is to decrease the eluent consumption (or eluent recovery duty), then the OSS *extract-raffinate* strategy seems to be the more indicated, since it will not affect the separation region too much but will in fact improve the efficiency of both sections I and IV.

Variants of OSS Technique

As mentioned before, the canonical name of 50–50% OSS *raffinate-extract* was given to describe a technique where the extract port is closed during the first half of the switching time, while the less retained product is being collected on the raffinate stream, and for the rest of the switching time period the raffinate port is closed while the more retained species is being collected on the extract stream, and vice-versa for the 50–50% OSS *extract-raffinate* mode of operation. However, and for example, in the case of the OSS *extract-raffinate* mode of operation, one could operate it during the initial 30% of the switching time period collecting the more retained product in the extract and last 30% period of the switching time withdrawing the less retained species in the raffinate (in the remaining time both ports are closed), what would be the 30–30% OSS *extract-raffinate* strategy; in the same way one could just operate the OSS strategy in the extract port closing the extract port for the final 50% of the switching time period (50% OSS *extract-0*) or closing it in the initial 50% period (50% OSS *0-extract*), and similarly for the raffinate port (50% OSS *raffinate-0* ...). One will now study these variants in particular and thus detailing the influence of the closing period as well as the extract or the raffinate influence per se.

For the sake of simplicity just the OSS *extract-raffinate* technique, which presented better results in terms of eluent consumption, will now be studied and in particular the OSS *extract-0* and OSS *0-raffinate* variants.

OSS Extract-0. Under the scope of the OSS operating technique, closing and opening the extract port means that only the flow rate in section I will suffer variations. Thus, the influence of this variant technique (OSS *extract-0*) and the collecting time in Q_I^* is now analyzed by means of successive simulations in the case of guaifenesin separation with $Q_{II}^* = 36.2\,\mathrm{ml \cdot min^{-1}}$, $Q_{III}^* = 37.1\,\mathrm{ml \cdot min^{-1}}$, $Q_{IV}^* = 32.5\,\mathrm{ml \cdot min^{-1}}$, and $t_s = 2.57\,\mathrm{min}$, Table 3.

As can be observed from Table 3, when comparing OSS *extract-0* with the classic SMB operating modes, the difference in the extract purity is almost insignificant (but better in the classic SMB mode of operation); however, the raffinate purity values obtained by the classic SMB mode of operation are always lower than the ones obtained when running with the OSS *extract-0* operating mode, independently of the collecting time period. Within the OSS *extract-0* operating strategy and for a given Q_I^* flow rate value, the extract purity value increases with the collecting period, but in a minor extension to what it is observed in the raffinate purities, where the higher purity values are observed for the lower collecting periods. However, one should remember that the shorter the collecting period is, the higher will be the extract flow rate during this period and thus the perturbations in the system, which can play a relevant role in the practical implementation of the OSS technique.

As mentioned before, the OSS *extract-0* operating strategy mainly influences the front section I. By operating in OSS *extract-0*, the more retained species front in section I will suffer a contraction and thus avoiding this product to move with the solid to section IV when the ports switching operation is performed. It is then possible to achieve

TABLE 3
OSS *extract-0* analysis: collecting time and Q_I^*, for $Q_{II}^* = 36.2\,\text{ml}\cdot\text{min}^{-1}$, $Q_{III}^* = 37.1\,\text{ml}\cdot\text{min}^{-1}$, $Q_{IV}^* = 32.5\,\text{ml}\cdot\text{min}^{-1}$, and $t_s = 2.57\,\text{min}$

Q_I^* ($\text{ml}\cdot\text{min}^{-1}$)	Extract Purity (PU_X, %)					
	30% OSS *X0*	40% OSS *X0*	50% OSS *X0*	60% OSS *X0*	70% OSS *X0*	Classic
40.5	99.98	99.99	100.00	100.00	100.00	100.00
41.0	99.96	99.97	99.98	99.99	99.99	100.00
41.5	99.95	99.96	99.97	99.98	99.98	100.00
42.0	99.95	99.95	99.96	99.97	99.97	99.99
42.5	99.94	99.95	99.96	99.97	99.97	99.98
43.0	99.94	99.95	99.96	99.96	99.97	99.98
Q_I^* ($\text{ml}\cdot\text{min}^{-1}$)	Raffinate Purity (PU_R, %)					
	30% OSS *X0*	40% OSS *X0*	50% OSS *X0*	60% OSS *X0*	70% OSS *X0*	Classic
40.5	94.95	94.80	94.60	94.36	94.04	92.42
41.0	97.61	97.48	97.31	97.09	96.81	95.33
41.5	99.14	99.05	98.93	98.78	98.57	97.44
42.0	99.79	99.74	99.69	99.61	99.49	98.78
42.5	99.96	99.95	99.93	99.90	99.86	99.51
43.0	100.00	99.99	99.99	99.98	99.97	99.83

higher raffinate purities operating under OSS *extract-0* or, reduce the eluent consumption for a given raffinate purity requirement, as shown in Fig. 5.

The shorter the collecting time period is, the higher will be the front compression and thus, the potential of the operating technique.

OSS 0-Raffinate. In opposition to what happens with the OSS *extract-0* strategy, by closing and opening the raffinate port it will only affect the flow rate in section IV since the eluent flow rate compensates the remaining flow rates (namely in section I and by consequence sections II and III). Thus, the influence of OSS *0-raffinate* variant technique versus Q_{IV}^* and the collecting time is now analyzed, again by running successive simulations on the case of guaifenesin separation by keeping constants: $Q_{II}^* = 36.2\,\text{ml}\cdot\text{min}^{-1}$, $Q_{III}^* = 37.1\,\text{ml}\cdot\text{min}^{-1}$, $Q_I^* = 37.1\,\text{ml}\cdot\text{min}^{-1}$, and $t_s = 2.57\,\text{min}$, Table 4.

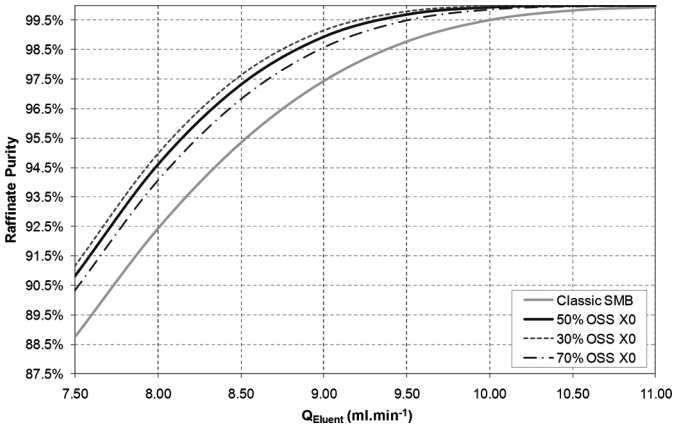

FIG. 5. Eluent consumption *vs.* raffinate purity for Classic SMB and OSS *X0* operating modes.

From Table 4, it can be observed that the difference in the raffinate purities between the OSS *0-raffinate* and the classic SMB operating modes is small, but worse in the classic SMB mode of operation case; nevertheless, the extract purities in the classic SMB mode of operation are always lower than the ones obtained when running with the OSS *0-raffinate* operating mode, independently of the collecting time period.

Within the OSS *0-raffinate* operating strategy, and for a given Q_{IV}^* flow rate value, the purity values (extract and raffinate) increase as the collecting period decreases. Again, one should remember the practical consequences of operating at low collecting periods mentioned before.

The same justification given to the front contraction in section I when operating under the OSS *extract-0* strategy, can now be applied to section IV, where the less retained species front is compressed by operating under the OSS *0-raffinate* technique. Once again, it is possible to either

TABLE 4
OSS *0-raffinate* analysis: collecting time and Q_{IV}^*, for $Q_{II}^* = 36.2\,\text{ml}\cdot\text{min}^{-1}$, $Q_{III}^* = 37.1\,\text{ml}\cdot\text{min}^{-1}$, $Q_I^* = 42.5\,\text{ml}\cdot\text{min}^{-1}$, and $t_s = 2.57\,\text{min}$

Q_{IV}^* ($\text{ml}\cdot\text{min}^{-1}$)	Extract Purity (PU_X, %)					
	30% OSS *0R*	40% OSS *0R*	50% OSS *0R*	60% OSS *0R*	70% OSS *0R*	Classic
34.625	99.98	99.98	99.98	99.98	99.98	99.77
34.750	99.98	99.98	99.98	99.97	99.95	99.55
34.875	99.98	99.98	99.97	99.95	99.90	99.10
35.000	99.97	99.96	99.94	99.89	99.79	98.18
35.125	99.94	99.90	99.83	99.68	99.39	96.39
35.250	97.54	97.53	97.51	97.41	97.11	93.45
Q_{IV}^* ($\text{ml}\cdot\text{min}^{-1}$)	Raffinate Purity (PU_R, %)					
	30% OSS *0R*	40% OSS *0R*	50% OSS *0R*	60% OSS *0R*	70% OSS *0R*	Classic
34.625	99.80	99.80	99.79	99.79	99.68	99.68
34.750	99.81	99.80	99.80	99.79	99.78	99.70
34.875	99.81	99.81	99.80	99.80	99.79	99.71
35.000	99.82	99.81	99.81	99.80	99.79	99.72
35.125	99.82	99.82	99.81	99.81	99.80	99.73
35.250	99.83	99.83	99.82	99.82	99.81	99.75

improve extract purities or reduce the eluent consumption for a given extract purity requirement, Fig. 6.

By compressing both fronts (the more retained species in section I and the less retained species in section IV) it is then possible to experience the OSS technique at its complete potential, i.e., couple the advantage of each variant in a single operating procedure OSS *extract-raffinate* (for instance, OSS *extract-0,* to decrease the flow rate to section I and OSS *0-raffinate* to increase the recycle flow rate, decreasing the eluent consumption).

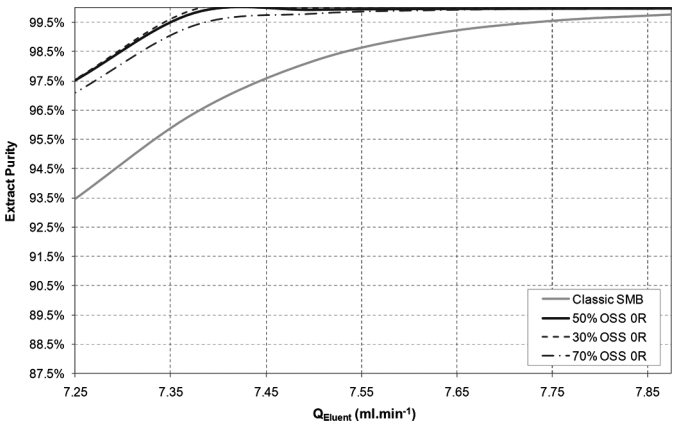

FIG. 6. Eluent consumption *vs.* extract purity for Classic SMB and OSS *0R* operating modes.

EXPERIMENTAL SECTION

With the FlexSMB-LSRE® unit detailed elsewhere (20) it is possible to run the OSS-*X0* mode of operation (or OSS-*0R*, by placing the extract pump in the raffinate outlet). However, the problems associated with recycle flow rate instability, noted in the classic SMB mode of operation (20), could be more critical when operating under the OSS *modus operandi*. The flow rates' variations due to the OSS mode of operation, would lead to a considerable increase of the recycle flow rate instability. Therefore, the unit was improved by changing the place of the recycle pump, initially positioned next to the extract node (in the beginning of section II), to the recycle line next to the raffinate node (beginning of section IV). The flow meter was changed to the previous position of this pump, i.e., next to the extract node (in the beginning of section II). This alteration led to a new pumps arrangement for the FlexSMB-LSRE® unit, Fig. 7.

In this way it was possible to avoid the mentioned instabilities, as well as a constant average value in the internal flow rates along a complete cycle, Fig. 8.

From Fig. 8, it is possible to observe that the new position of the recycle pump (next to the raffinate node or the beginning of section IV), allowed a considerable stability in the internal flow rates (now measured by the flow meter installed next to the extract node). The two different amplitudes noted for the flow rate oscillation within each switching time period noted in Fig. 8, are directly related

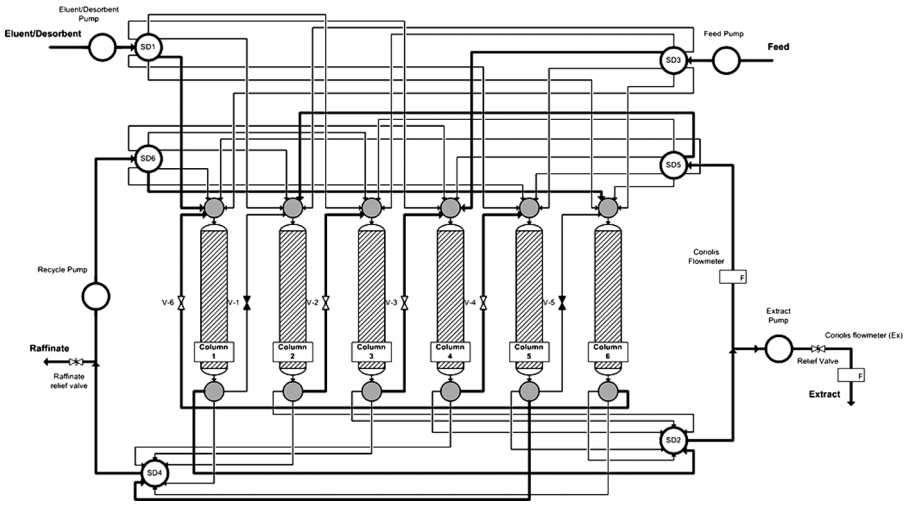

FIG. 7. FlexSMB-LSRE® pumps and valves scheme developed to avoid recycle flow rate asymmetries.

to the particularities of the 60% OSS *X0* mode of operation. The amplitude oscillation for the first part of the switching time is higher than the second, probably related with the fact that the flow meter (coriolis) has been just zeroed for the second part of the OSS operating mode.

At the same time, some dead volumes associated with the connections of both the flow meter and the recycle pump were reduced, by using 1 mm *i.d.* stainless steel capillary tubes which were before Teflon tubes, Table 5.

The values given in Table 5 include also the contribution of all the stagnant volumes. Considering only the active lines (see Fig. 7), the dead volumes for each section are: $V_I^D = 1.09\,\text{ml}$; $V_{II}^D = 3.84\,\text{ml}$; $V_{III}^D = 1.71\,\text{ml}$; $V_{IV}^D = 4.73\,\text{ml}$, which led to a new dead volumes and switching time compensation measure of 2.60% (see (20) for further details on the dead volumes compensation strategy of the FlexSMB-LSRE® unit).

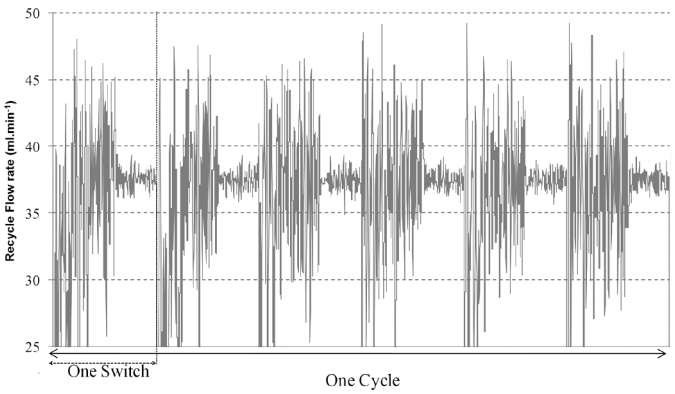

FIG. 8. Flow rate in the beginning of section II, after the unit alteration; FlexSMB-LSRE® operating in 60% OSS *X0* mode.

Operating Conditions

For the OSS experiment, the variant 60% OSS *X0* was chosen to introduce the minimal flow rate oscillations and to fit the $\frac{1}{5}t_s$ discretization of the switching time period allowed by the FlexSMB-LSRE® operating routines.

The operating conditions observed during the OSS experiment are presented in Table 6.

The average operating conditions are presented in Table 7.

Sampling and Analytical Procedures

The internal concentration profiles at the Cyclic Steady State (CSS) were withdrawn by means of the 6-port valve

TABLE 5
Dead volumes per function and total dead volumes percentage in the FlexSMB-LSRE® unit, after unit re-arrangement and dead volumes reduction

	V_{each}(ml)	Total
Filter and manifold	0.50	3.01
Ext in	0.36	2.17
Raf in	0.36	2.17
Ext out	0.32	1.93
Raf out	0.32	1.93
Interc	0.31	1.89
Sampler	0.47	0.47
Ext 1	0.12	0.12
Ext 2 (flow meter)	2.29	2.29
Raf 1	0.12	0.12
Raf 2 (Rec pump)	3.79	3.79
V_c (ml)		188.5
(%) dead volumes		11.0%

TABLE 6
Experimental operating conditions for the guaifenesin racemic mixture separation operated under the 60% OSS *X0* -SMB

Step 1 from 0 to $0.6t_s$- SMB operating conditions (measured)			
$Q_I^* = 47.7\,\mathrm{ml \cdot min^{-1}}$		Eluent	$14.9\,\mathrm{ml \cdot min^{-1}}$
$Q_{II}^* = 36.4\,\mathrm{ml \cdot min^{-1}}$		Extract	$11.3\,\mathrm{ml \cdot min^{-1}}$
$Q_{III}^* = 37.3\,\mathrm{ml \cdot min^{-1}}$		Feed	$0.9\,\mathrm{ml \cdot min^{-1}}$
$Q_{IV}^* = 32.8\,\mathrm{ml \cdot min^{-1}}$		Raffinate	$4.5\,\mathrm{ml \cdot min^{-1}}$
$t_s = 2.64\,\mathrm{min}$			
$\gamma_I^*\Big\vert_{FlexSMB} = 10.02$	$\gamma_{II}^*\Big\vert_{FlexSMB} = 7.65$	$\gamma_{III}^*\Big\vert_{FlexSMB} = 7.84$	$\gamma_{IV}^*\Big\vert_{FlexSMB} = 6.90$
Step 2 from $0.6t_s$ to t_s- SMB operating conditions (measured)			
$Q_I^* = 36.7\,\mathrm{ml \cdot min^{-1}}$		Eluent	$3.9\,\mathrm{ml \cdot min^{-1}}$
$Q_{II}^* = 36.7\,\mathrm{ml \cdot min^{-1}}$		Extract	$0\,\mathrm{ml \cdot min^{-1}}$
$Q_{III}^* = 37.6\,\mathrm{ml \cdot min^{-1}}$		Feed	$0.9\,\mathrm{ml \cdot min^{-1}}$
$Q_{IV}^* = 32.8\,\mathrm{ml \cdot min^{-1}}$		Raffinate	$4.8\,\mathrm{ml \cdot min^{-1}}$
$t_s = 2.64\,\mathrm{min}$			
$\gamma_I^*\Big\vert_{FlexSMB} = 7.71$	$\gamma_{II}^*\Big\vert_{FlexSMB} = 7.71$	$\gamma_{III}^*\Big\vert_{FlexSMB} = 7.90$	$\gamma_{IV}^*\Big\vert_{FlexSMB} = 6.90$

at 25%, 50%, and 75% of the switching time and extract and raffinate ports, and samples of the extract and raffinate average concentrations were collected at each cycle.

All the analyses were performed by means of an HPLC system, which includes a Smartline 1000 LC pump, UV detector model Smartline 2500, LPG block and degasser (Knauer, Germany). The detector was set at 270 nm and a Rheodyne injection valve with a 10 μL sample loop was loaded manually using a syringe. Clarity (DataApex, Ltd., 2004) software was used for data acquisition and HPLC control. The analytical was column (250 mm × 4.6 mm I.D.) packed with Chiralpak IB: cellulose tris (3,5 dimethylphenylcarbamate immobilized onto 5 μm silica-gel), supplied by Chiral Technologies Europe (France) was used. GC-grade organic solvents *n*-heptane and ethanol (EtOH) were obtained from Sigma-Aldrich Chemie, Germany. The antitussive drug guaifenesin was dissolved in the mobile phase which was always degassed and filtrated through a 0.2 μm, 50 mm I.D. NL 16-membrane filter (Schleicher & Schuell, Germany) before use. The mobile phase was *n*-heptane/ethanol (85/15%, v/v).

RESULTS AND DISCUSSION

During the first run of the OSS experiment some problems were noted (instability in the flow rates measurement), which led to the reformulation of the unit. After the reformulation of the unit, the parameters were again set on the computer interface and the unit operated for more than 50 cycles (continuing the profiles from the first experiment). The average concentration history, as well as the purities, in the extract and raffinate ports for the last 10 cycles (40 to 50) are shown in Fig. 9.

TABLE 7
Average experimental operating conditions for the guaifenesin racemic mixture separation operated under the 60% OSS *X0* -SMB

SMB operating conditions (Average)			
$Q_I^* = 43.3\,\mathrm{ml \cdot min^{-1}}$		Eluent	$10.5\,\mathrm{ml \cdot min^{-1}}$
$Q_{II}^* = 36.5\,\mathrm{ml \cdot min^{-1}}$		Extract	$6.8\,\mathrm{ml \cdot min^{-1}}$
$Q_{III}^* = 37.4\,\mathrm{ml \cdot min^{-1}}$		Feed	$0.9\,\mathrm{ml \cdot min^{-1}}$
$Q_{IV}^* = 32.8\,\mathrm{ml \cdot min^{-1}}$		Raffinate	$4.6\,\mathrm{ml \cdot min^{-1}}$
$t_s = 2.64\,\mathrm{min}$			
$\gamma_I^*\Big\vert_{FlexSMB} = 8.87$	$\gamma_{II}^*\Big\vert_{FlexSMB} = 7.68$	$\gamma_{III}^*\Big\vert_{FlexSMB} = 7.86$	$\gamma_{IV}^*\Big\vert_{FlexSMB} = 6.90$

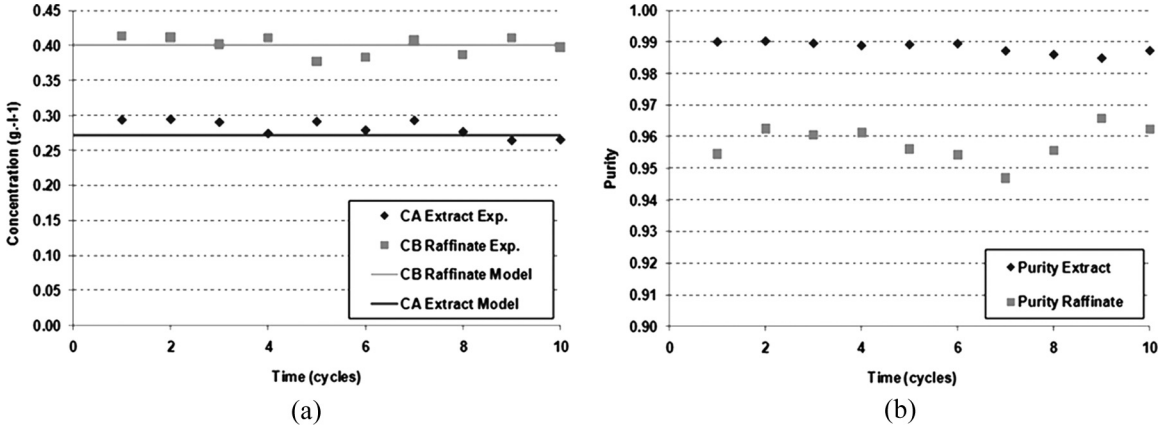

FIG. 9. (a) Average concentration history, (b) purities in the extract and raffinate ports from cycle 40 to 50; lines the simulated values (average over a cycle).

As can be observed in Fig. 9, at this stage (from cycle 40 to 50) the unit was already in/near the CSS (mass balance closed (+/−3%) for each species).

The internal concentration profiles obtained from the sampling procedure at 25%, 50%, and 75% of the switching time are presented in Fig. 10.

The simulated profiles in Figs. 9 and 10, as well as all the following results, were calculated by means of an extended mathematical model considering all the FlexSMB-LSRE® dead volumes, switching asymmetries as dead volumes compensating measures, as detailed elsewhere (20).

The average purity values for both the more retained product in the extract and less retained species in the raffinate ports are reported in Table 8.

Nevertheless, it can be noted that some difference exists between the simulated and experimental purity results in both extract and raffinate streams, Table 8. Also some experimental points in the internal concentration profile shown in Fig. 8, are not coincident with those predicted by the detailed model. A possible reason on these discrepancies can be related with an overestimation of the mass transfer coefficient, $k_{\text{int}} = 0.20\,\text{cm}\cdot\text{min}^{-1}$, calculated by correlation (see section 2.1). Particular attention was given to this aspect and a new estimative was found that would better fit the experimental data: $k_{\text{int}} = 0.07\,\text{cm}\cdot\text{min}^{-1}$. By simulating with this value one can now find the following internal concentration profiles in Fig. 11 and the performance parameters in Table 9.

One can observe in Fig. 11 that the simulated values obtained by considering $k_{\text{int}} = 0.07\,\text{cm}\cdot\text{min}^{-1}$ are closer to the experimental ones. Even though the results cannot be directly compared with the classical experiment presented before (different operating conditions), it is possible to compare the simulated result obtained for the OSS *X0* simulation (with $k_{\text{int}} = 0.07\,\text{cm}\cdot\text{min}^{-1}$) with the ones that would be obtained by running the correspondent classical mode of operation (also considering $k_{\text{int}} = 0.07\,\text{cm}\cdot\text{min}^{-1}$), Fig. 12 and Table 10.

As can be observed from Fig. 12, just the concentration profile around the extract port will change considerably. From Table 10, it can be noted that if one operates under

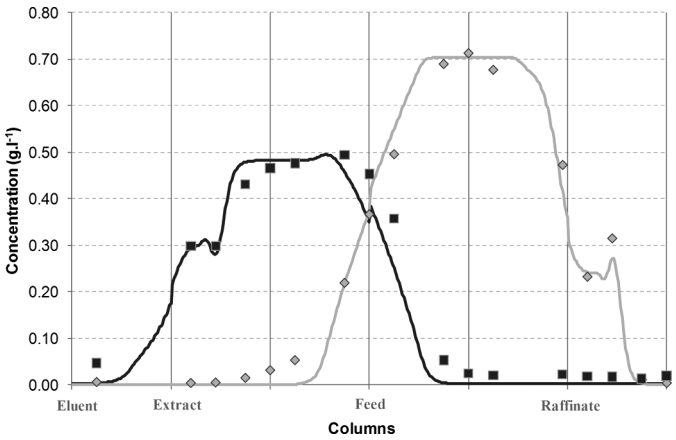

FIG. 10. Experimental internal concentration profile at half switching time period operating OSS-*X0* SMB; black squares representing experimental C_{b_A}, grey diamonds the experimental C_{b_B}; the black line the simulated C_{b_A} and the grey line the simulated C_{b_B}.

TABLE 8
Experimental and simulated purity values for the more retained product in the extract and less retained one in the raffinate

	Simulated		Experimental	
	extract	raffinate	extract	raffinate
Purity (%)	99.99	99.59	98.83	95.81
Recovery (%)	99.59	99.99	96.10	98.24

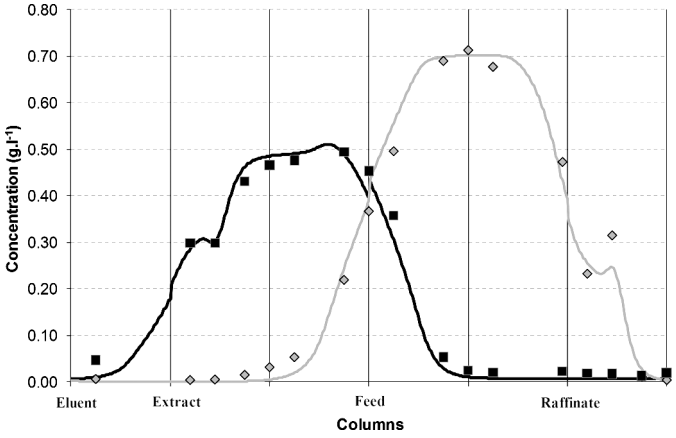

FIG. 11. Experimental internal concentration profile at half switching time period after 10 cycles operating as OSS *X0* SMB; black squares representing experimental C_{b_A}, grey diamonds the experimental C_{b_B}; the black line the simulated C_{b_A} and the grey line the simulated C_{b_B}, both considering $k_{\text{int}} = 0.07\,\text{cm}\cdot\text{min}^{-1}$.

TABLE 9
Experimental and simulated (considering $k_{\text{int}} = 0.07\,\text{cm}\cdot\text{min}^{-1}$) purity values for the more retained product in the extract and less retained one in the raffinate

	Simulated		Experimental	
	extract	raffinate	extract	raffinate
Purity (%)	99.80	98.63	98.83	95.81
Recovery (%)	98.62	99.80	96.10	98.24

the classic SMB both the raffinate as extract purities will be more reduced, when compared with the OSS *X0* operating strategy. Both observations converge to the same conclusion: as expected the contraction of the front of the more retained component in section I and II (near the extract port), consequence of the OSS *X0* operating mode, will allow a better separation (better purity values) than the ones observed if one runs under the classic mode of operation, but at the cost of more operational instability.

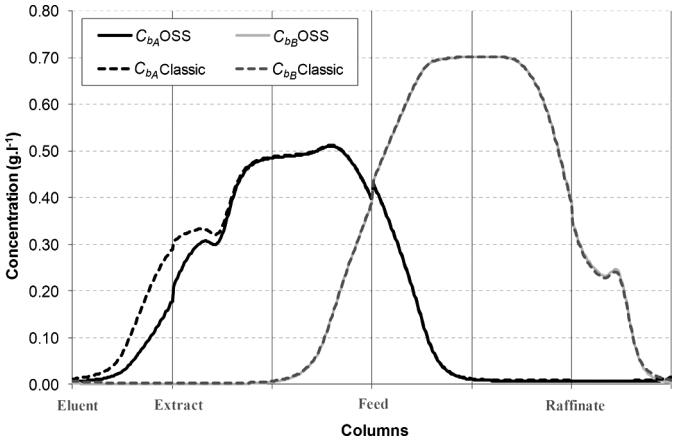

FIG. 12. Bulk concentration profile at half switching both OSS *X0* and Classic SMB modes of operation, both considering $k_{\text{int}} = 0.07\,\text{cm}\cdot\text{min}^{-1}$.

TABLE 10
Purity values for the more retained product in the extract and less retained one in the raffinate for the OSS *X0* and Classic SMB modes of operation, both considering $k_{\text{int}} = 0.07\,\text{cm}\cdot\text{min}^{-1}$

	OSS-X0		Classic	
	extract	raffinate	extract	raffinate
Purity (%)	99.80	98.63	98.85	98.30
Recovery (%)	98.62	99.80	98.30	98.85

CONCLUSIONS

A detailed methodology, based on the systematic simulation of the complete separation as regeneration regions, was undertaken to study the non-conventional SMB technique: Outlet Streams Swing (OSS). By these means, it was possible to extend further the comprehension of the impact of the periodical outlet collection procedure, specific to the OSS technique, on the performance of such non-conventional SMB operating mode.

It was shown, by means of the OSS technique, that the compression or expansion movements in both the less retained species front in section IV and the more retained component in section I, can be adjusted either:

1. to increase the separation region and thus improving the unit productivity for given purity requirements (achieved when operating under OSS raffinate-extract strategy); or,
2. to decrease the eluent consumption (possible by operating under OSS extract-raffinate strategy).

Different variants of the OSS technique were also studied, detailing the influence of intrinsic parameters of the OSS strategy, such as the collecting period and presenting more simplistic applications of the OSS technique. One of these variants, the 60% OSS *X0*, was experimentally demonstrated, stating its operability, as well as the common drawbacks that most of the non-conventional SMB techniques based on flow rates variation usually presents (instabilities in the internal flow rates and considerable time required to reach the CSS).

Following the methodology developed in this work, it will be possible to extend further the potentialities of these

kinds of operating modes (for instance, by coupling the OSS technique with the partial feed operating strategy), and to better understand other generic non-conventional techniques.

ACKNOWLEDGEMENTS

Pedro Sá Gomes gratefully acknowledges the support from ''Fundação para a Ciência e Tecnologia'', Ministry of Science, Technology and Higher Education of Portugal (SFRH/BD/22103/2005 PhD grant). Part of this work is based on the oral presentation in: AICHE - 2009 Annual Meeting, Nashville TN-USA by Sá Gomes, P., Silva, V.M.TM., Rodrigues, A.E (2009). The Outlet Streams Swing Simulated Moving Bed Mode of Operation.

NOMENCLATURE

C_b	bulk liquid phase concentration ($g \cdot l^{-1}$)
$\overline{C_p}$	particle pore average concentration ($g \cdot l^{-1}$)
d	diameter (m)
D_b	axial dispersion coefficient in packed bed ($cm^2 \cdot min^{-1}$)
D_m	molecular diffusivity ($cm^2 \cdot min^{-1}$)
K	adsorption equilibrium constant ($l \cdot g^{-1}$)
k_{int}	internal mass transfer coefficient ($cm \cdot min^{-1}$)
L	length (m)
M	molar mass of the solute ($g \cdot mol^{-1}$)
q^{eq}	equilibrium adsorbed concentration ($g \cdot l^{-1}_{\text{adsorbent}}$)
q_m	adsorbed phase saturation concentration ($g \cdot l^{-1}_{\text{adsorbent}}$)
Q	liquid flow rate ($ml \cdot min^{-1}$)
T	temperature (K)
t	time variable (min)
t_s	switching time (min)
u	interstitial velocity ($cm \cdot min^{-1}$)
V	volume (l)
V_m	molar volume of the adsorbate at its normal boiling temperature ($l \cdot mol^{-1}$)
z	axial variable (cm)

Greek Letters

ε_b	bulk porosity (-)
ε_p	internal porosity (-)
ϕ	association factor (-)
μ	viscosity (Pa.s)
τ	tortuosity (-)

Subscripts and Superscripts

eq	equilibrium
i	species in binary system
j	number of section ($j = \text{I,II,III,IV}$)
k	number of column ($k = 1,2,\ldots 6$)
c	column
p	particle
*	operating conditions in SMB
E, F, R, X	eluent, feed, raffinate, extract SMB stream

Abbreviations

CSS	Cyclic Steady State
ISMB	Improved Simulated Moving Bed
LDF	Linear Driving Force
OSS	Outlet Stream Swing
PR	Productivity
PU	Purity
RE	Recovery
SMB	Simulated Moving Bed
TMB	True Moving Bed

REFERENCES

1. Broughton, D.B.; Neuzil, R.W.; Pharis, J.M.; Brearley, C.S. (1970) The Parex process for recovering paraxylene. *Chemical Engineering Progress*, 66 (9): 70–75.
2. Broughton, D.B.; Gerhold, C.G. (1961) Continuous Sorption Process Employing Fixed Bed of Sorbent and Moving Inlets and Outlets. U.S. Patent No. 2,985,589.
3. Seidel-Morgenstern, A.; Keßler, L.C.; Kaspereit, M. (2008) New developments in simulated moving bed chromatography. *Chemical Engineering and Technology*, 31 (6): 826–837.
4. Sá Gomes, P. (2009) Advances in Simulated Moving Bed: New operating modes; New design methodologies; and Product (FlexSMB-LSRE) development, PhD Thesis - Laboratory of Separation and Reaction Engineering, Faculty of Engineering of the University of Porto: Porto.
5. Sá Gomes, P.; Minceva, M.; Pais, L.S.; Rodrigues, A.E. (2007) Advances in simulated moving bed chromatographic separations. In: *Chiral Separation Techniques*, 3rd Ed.; Dr. Ganapathy, S., ed.; 181–202.
6. Sá Gomes, P.; Minceva, M.; Rodrigues, A.E. (2006) Simulated moving bed technology: Old and new. *Adsorption*, 12 (5–6): 375–392.
7. Rajendran, A.; Paredes, G.; Mazzotti, M. (2009) Simulated moving bed chromatography for the separation of enantiomers. *Journal of Chromatography A*, 1216 (4): 709–738.
8. Zang, Y.; Wankat, P.C. (2002) SMB operation strategy - partial feed. *Industrial and Engineering Chemistry Research*, 41 (10): 2504–2511.
9. Zang, Y.; Wankat, P.C. (2002) Three-zone simulated moving bed with partial feed and selective withdrawal. *Industrial and Engineering Chemistry Research*, 41 (21): 5283–5289.
10. Kloppenburg, E.; Gilles, E.D. (1999) A new concept for operating simulated moving-bed processes. *Chemical Engineering and Technology*, 22 (10): 813–817.
11. Zhang, Z.; Mazzotti, M.; Morbidelli, M. (2003) PowerFeed operation of simulated moving bed units: Changing flow-rates during the switching interval. *Journal of Chromatography A*, 1006 (1–2): 87–99.
12. Kawajiri, Y.; Biegler, L.T. (2006) Optimization strategies for simulated moving bed and powerfeed processes. *AIChE Journal*, 52 (4): 1343–1350.
13. Zhang, Z.; Morbidelli, M.; Mazzotti, M. (2004) Experimental assessment of PowerFeed chromatography. *AIChE Journal*, 50 (3): 625–632.
14. Bae, Y.S.; Lee, C.H. (2006) Partial-discard strategy for obtaining high purity products using simulated moving bed chromatography. *Journal of Chromatography A*, 1122 (1–2): 161–173.

15. Keßler, L.C.; Seidel-Morgenstern, A. (2008) Improving performance of simulated moving bed chromatography by fractionation and feedback of outlet streams. *Journal of Chromatography A*, 1207 (1–2): 55–71.
16. Lutin, F.; Bailly, M.; Bar, D. (2002) Process improvements with innovative technologies in the starch and sugar industries. *Desalination*, 148 (1–3): 121–124.
17. Katsuo, S.; Mazzotti, M. (2010) Intermittent simulated moving bed chromatography: 1. Design criteria and cyclic steady-state. *Journal of Chromatography A*, 1217 (8): 1354–1361.
18. Sá Gomes, P.; Rodrigues, A.E. (2007) Outlet Streams Swing (OSS) and MultiFeed operation of simulated moving beds. *Separation Science and Technology*, 42 (2): 223–252.
19. Sá Gomes, P.; Silva, V.M.T.; Rodrigues, A.E. (2009) *The Outlet Streams Swing Simulated Moving Bed Mode of Operation*, in AICHE Annual Meeting: Nashville-TN, USA.
20. Sá Gomes, P.; Zabkova, M.; Zabka, M.; Minceva, M.; Rodrigues, A.E. (2010) Separation of chiral mixtures in real SMB units: The FlexSMB-LSRE®. *AIChE Journal*, 56 (1): 125–142.
21. Glueckauf, E. (1955) Theory of chromatography. Part 10. Formulae for diffusion into spheres and their application to chromatography. *Trans. Faraday Soc.*, 51: 1540–1551.
22. Wilke, C.R.; Chang, P. (1955) Correlation of diffusion coefficients in dilute solutions. *AIChE Journal*, 1 (2): 264–270.
23. Perkins, L.R.; Geankoplis, C.J. (1969) Molecular diffusion in a ternary liquid system with the diffusing component dilute. *Chemical Engineering Science*, 24 (7): 1035–1042.
24. Teja, A.S.; Rice, P. (1981) Generalized corresponding states method for the viscosities of liquid mixtures. *Industrial and Engineering Chemistry Fundamentals*, 20 (1): 77–81.
25. Danckwerts, P.V. (1953) Continuous flow systems: Distribution of residence times. *Chemical Engineering Science*, 2 (1): 1–13.
26. Storti, G.; Mazzotti, M.; Morbidelli, M.; Carra, S. (1993) Robust design of binary countercurrent adsorption separation processes. *AIChE Journal*, 39 (3): 471–492.
27. Azevedo, D.C.S.; Rodrigues, A.E. (1999) Design of a simulated moving bed in the presence of mass-transfer resistances. *AIChE Journal*, 45 (5): 956–966.